JOC The Journal of Organic Chemistry

Article

pubs.acs.org/joc

Stone–Wales Rearrangements in Hydrocarbons: From Planar to Bowl-Shaped Substrates

Erica E. Irace,[†] Evangelina Brayfindley,[†] Gail A. Vinnacombe,[†] Claire Castro,*[,†] and William L. Karney*[,†,‡]

[†]Department of Chemistry and [‡]Department of Environmental Science, University of San Francisco, 2130 Fulton Street, San Francisco, California 94117 United States

Supporting Information

ABSTRACT: Carbene, cyclobutyl, and potential diradical mechanisms were studied computationally for Stone–Wales rearrangements in several derivatives of *as*-indacene and pyracyclene, including cyclopent[*hi*]acephenanthrylene, dicyclopenta[*cd,fg*]pyrene, corannulene, diindeno[1,2,3,4-*defg*;1′,2′,3′,4′-*mnop*]-chrysene, and semibuckminsterfullerene. At the UM06-2X/cc-pVDZ and BD(T)/cc-pVDZ//UM06-2X/cc-pVDZ levels of theory, free energies of reaction reveal that transformations involving an increase in curvature are thermodynamically unfavorable. In addition, the carbene transition states or intermediates (corrected to 1000 °C) are generally around 100–120 kcal/mol higher than starting substrates, except for *as*-indacene (80 kcal/mol), which is the only process considered here that is predicted to have a barrier accessible under typical flash vacuum pyrolysis conditions. For pyracyclene derivatives, the relative free energy of cyclobutyl intermediates rises steadily with increasing curvature of the substrate and increasing annelation. Singlet acetylenic diradicals related to pyracyclene, diindenochrysene, and semibuckminsterfullerene are predicted to be second- or higher-order saddle points that lie more than 40 kcal/mol higher than the corresponding carbenes and cyclobutyl intermediates.

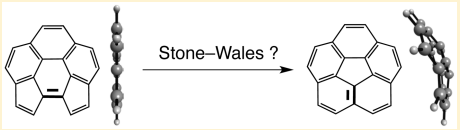

INTRODUCTION

The rearrangements of aromatic hydrocarbons at high temperatures[1] are relevant to many areas, including the formation of soot[2,3] and the synthesis of new carbon-rich materials.[4−7] Among the many fascinating transformations, perhaps one of the most elusive is the Stone–Wales rearrangement (SWR).[8] Originally proposed[8] as a formal way to relate the possible isomers of a given fullerene, the process consists of pairwise 1,2-shifts of C–C bonds, as shown in Scheme 1 for conversion

Scheme 1

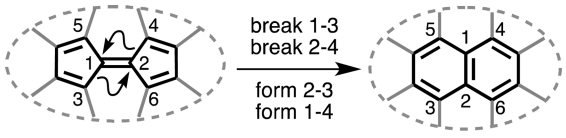

of a pentafulvalene to a naphthalene moiety. The net result is a 90° rotation of the central bond. Note that the curved arrows do not necessarily imply mechanism but rather simply show net changes in bonding.

Despite extensive study, direct evidence for Stone–Wales rearrangements is scarce. SWRs are assumed to operate during annealing of fullerenes,[9−11] and they likely occur during formation/repair of Stone–Wales defects in carbon nanotubes.[12,13] In smaller systems, Alder reported the conversion of bifluorenylidene (**1**) to dibenzo[*g,p*]chrysene (**2**),[14] and Vollhardt invoked Stone–Wales-like reactions (**3** → **4**, **6** → **7**, **7** → **8**) in explaining rearrangements of phenylenes under flash vacuum pyrolysis (FVP) conditions (Scheme 2).[15,16] For emphasis, the rotating C_2 unit in each substrate in Scheme 2 is shown in bold.

No experimental evidence exists for SWR in pyracyclene (**9**). At temperatures of 1000 °C and higher, **9** produces a mixture of ethynylacenaphthylenes and eliminates C_2 to yield acenaphthylene (Scheme 3).[17] ^{13}C labeling experiments by Scott showed that, at temperatures up to 1100 °C, pyracyclene (**9**) does not undergo SWR to move the labels from the five-membered rings into the six-membered rings (Scheme 3).[4] Nevertheless, some systems of interest here contain a pyracyclene subunit, so **9** serves as a useful reference point.

Other systems of interest here contain an *as*-indacene (**10**) subunit. Despite the fact that quinoidal species **10** has not been isolated,[18,19] the hypothetical SWR of **10** to acenaphthylene (**11**, Scheme 4) serves as another useful reference point for mechanisms and barriers.

Conceptually, perhaps the simplest mechanism for SWR involves in-plane rotation of the central C_2 unit via an acetylenic diradical transition state (**A**), as shown in Scheme 5 for pyracyclene. Stone and Wales noted[8] that such a concerted, dyotropic[20,21] mechanism is forbidden by orbital symmetry,[22] as shown for pyracyclene in the orbital diagram in Scheme 5. It involves four electrons in two simultaneous 1,2-shifts. The same conclusion—that the mechanism is forbidden—is also reached via other interpretations, such as viewing the interacting orbitals as a four-electron system with Hückel orbital topology.[23] Bettinger et al. reasoned, however, that orbital mixing involving the in-plane π MOs of the acetylenic moiety could explain why

Special Issue: 50 Years and Counting: The Woodward-Hoffmann Rules in the 21st Century

Received: June 5, 2015
Published: August 24, 2015

DOI: 10.1021/acs.joc.5b01274
J. Org. Chem. 2015, 80, 11718–11725

Scheme 2

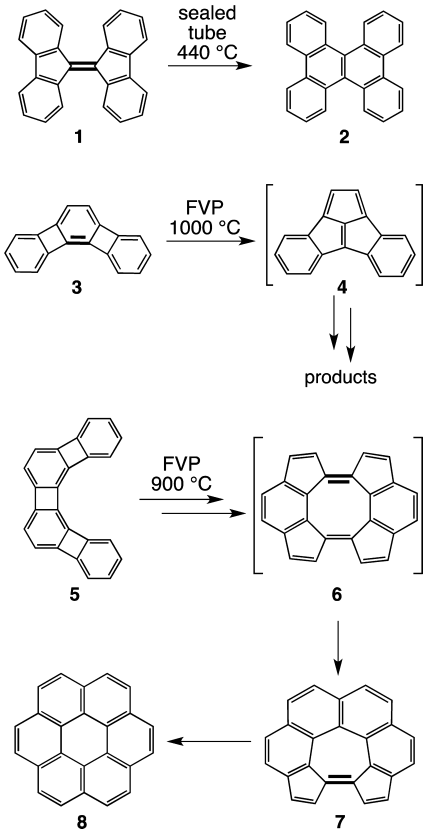

Scheme 3

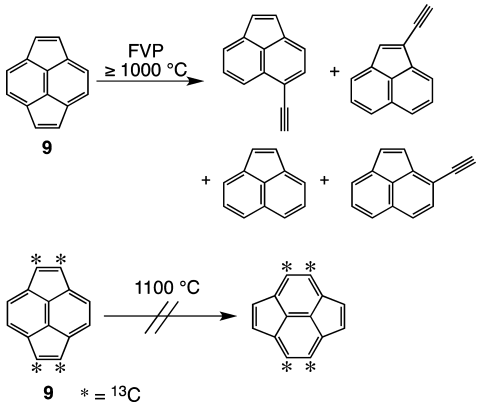

Scheme 4

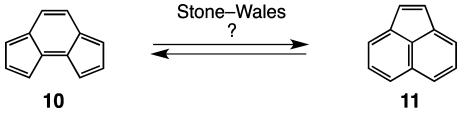

the diradical character of **A** is less than that implied by its Lewis structure.[12]

Prior theoretical work on SWRs has focused on the diradical mechanism in Scheme 5, as well as (i) a route via a cyclobutyl intermediate **B**, and (ii) a carbene mechanism (also sometimes called an sp^3 mechanism), in which the carbene **C** may be a transition state or an intermediate.[24] These latter two routes for pyracyclene are depicted in Scheme 6.

Scheme 5

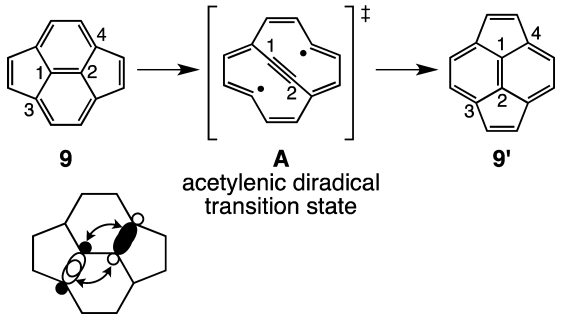

Scheme 6

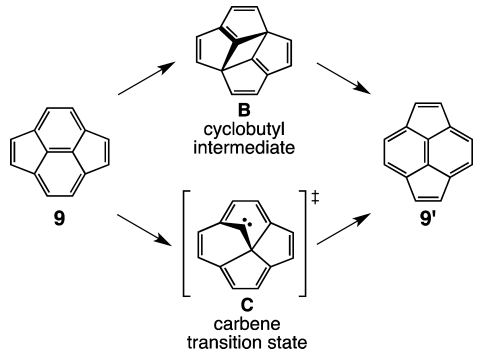

Bettinger reported DFT barriers of ~160 kcal/mol for the diradical and carbene mechanisms for SWR of C_{60}.[12] Alder located a carbene mechanism for **1** → **2** with an activation energy of 65 kcal/mol (B3LYP),[25] which is very similar to the recent BD(T) barrier found for that system.[26] Computed barriers for pyracyclene (**9**) range from 110 to 120 kcal/mol for the cyclobutyl pathway and from 130 to 143 kcal/mol for the carbene route.[26,27] Despite the high barrier for **9**, appropriate benzannelation of **9**, as in cyclopent[*fg*]aceanthrylene, is predicted to decrease the barrier for the cyclobutyl mechanism to as low as 87 kcal/mol.[26] CCSD(T) or BD(T) computed barriers for **3** → **4**, **6** → **7**, and **7** → **8**—none of which contain a pyracyclene subunit—range from 80 to 90 kcal/mol with carbene routes preferred in all three cases.[26,28]

It is worth noting that in the computed carbene transition state (**C**) for **9** in Scheme 6, the carbene carbon lies significantly above the average plane of the molecule, and the sp^3-hybridized carbon participates in three bonds that are nearly coplanar.[26,29] As a result, more highly bowl-shaped systems containing a pyracyclene subunit might more easily access such a nonplanar transition state and lower its relative energy accordingly.

Given how much activation energies and preferred mechanisms for SWR vary for different substrates, in this paper we aim to clarify how mechanism and barrier height depend on the amount of curvature (resulting from increasing annelation) in substrates and products, and on whether the substrate contains a pyracyclene or an *as*-indacene moiety. Here, we report computations on preferred mechanisms for SWR that systems might undergo to "avoid" the forbidden pathway and to point out trends as a function of core structure and degree of curvature. We also explore the possible involvement of acetylenic diradicals analogous to **A**. The substrates considered here range from flat species (e.g., **9** and **10**) up through significantly bowl-shaped 20- and 30-carbon species (corannulene and semibuckminsterfullerene), including several known hydrocarbons

DOI: 10.1021/acs.joc.5b01274
J. Org. Chem. 2015, 80, 11718−11725

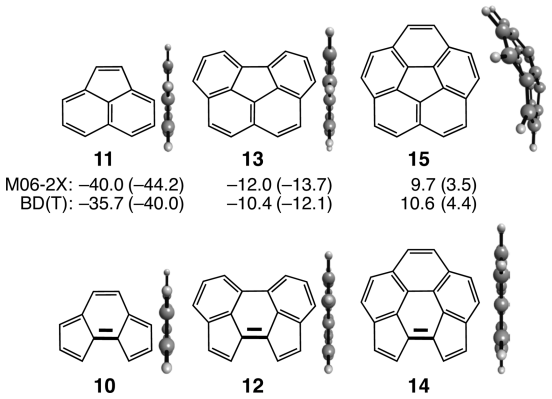

Figure 1. M06-2X/cc-pVDZ and BD(T)/cc-pVDZ//M06-2X/cc-pVDZ relative free energies (in kcal/mol, corrected to 1000 °C) of Stone–Wales reactants (bottom, set to 0.0) and products (top) for *as*-indacene derivatives. Values in parentheses are ZPE-corrected relative energies. Profile views (M06-2X/cc-pVDZ-optimized structures) are shown to the right of each species.

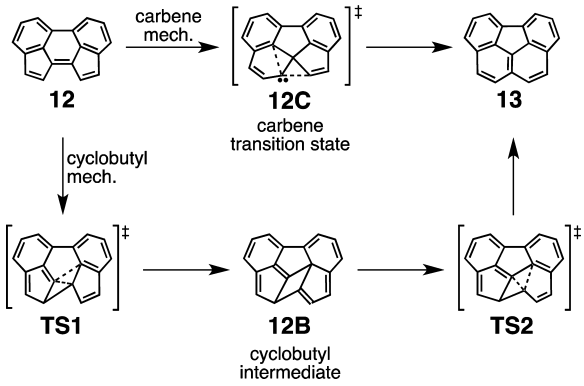

Figure 3. Carbene and cyclobutyl mechanisms located for the SWR of cyclopent[*hi*]acephenanthrylene (**12**) to benzo[*ghi*]fluoranthene (**13**).

of intermediate curvature between these extremes. Some of the substrates and products have been synthesized by pyrolytic routes, so calculations on high-temperature rearrangement mechanisms provide relevant perspective.

COMPUTATIONAL METHODS

Geometry optimizations were performed at the (U)M06-2X/cc-pVDZ level of theory.[30,31] Test calculations using a triple-ζ basis set, def2-TZVP,[32] showed that the resulting optimized structures yielded BD(T) relative energies that differed by <0.5 kcal/mol compared to energies obtained with the cc-pVDZ basis set. Details are provided in Table S1 in the Supporting Information. Vibrational analyses were carried out at the same level to verify the nature of stationary points. Transition states were confirmed by the presence of exactly one imaginary frequency, and the corresponding reaction paths were verified by intrinsic reaction coordinate (IRC) calculations. Vibrational analyses were employed to obtain zero-point energies, and also to obtain thermal corrections to the Gibbs free energy for all species, using a temperature of 1273 K—conditions that represent a reasonable approximation to the pyrolysis conditions previously reported for the reactions of interest. Thermal corrections were computed using unscaled vibrational frequencies and pertain to a pressure of 1.0 atm.

The use of unrestricted DFT was necessary to allow for possible diradical character in some species. Wave functions with broken spin symmetry were obtained by mixing the HOMO and LUMO. The $<S^2>$ values for most species were zero with only a few exceptions for carbenes (see Supporting Information). In the case of some acetylenic diradicals, open-shell singlet wave functions were generated using the guess = alter option in Gaussian 09, which results in a "50:50" wave function (50% singlet, 50% triplet).

Because of the presence of some singlet diradical character in some species, the Brueckner doubles method, BD(T),[33,34] with the cc-pVDZ basis set was employed for single point energies. Test calculations on the **9**/**9B** and **10**/**10C** pairs with larger basis sets (cc-pVTZ,[31] def2-TZVP,[32] def2-TZVPP,[32] aug-cc-pVTZ[35]) did not change the relative energies by more than 2 kcal/mol (see Tables S2 and S3 for details). Previous work on similar but smaller systems showed that BD(T)/cc-pVDZ relative energies agree well with those obtained at the CASPT2/cc-pVDZ level.[26] BD(T)/cc-pVDZ relative energies are reported as thermally corrected (1000 °C) Gibbs free energies. There may be significant uncertainties in the thermodynamic quantities

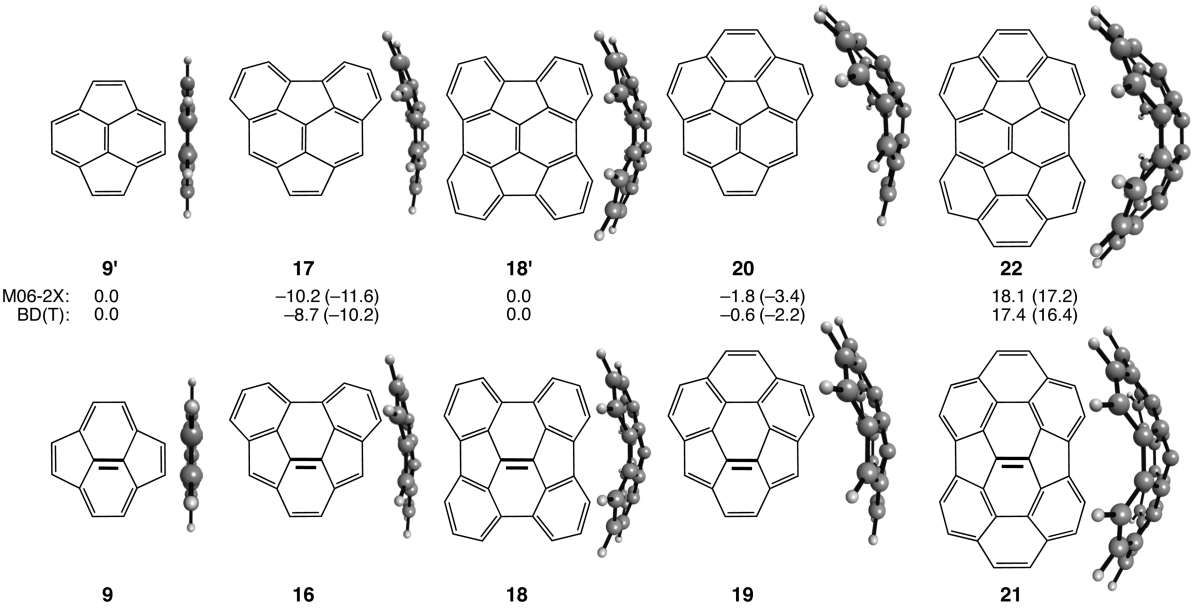

Figure 2. M06-2X/cc-pVDZ and BD(T)/cc-pVDZ//M06-2X/cc-pVDZ relative free energies (in kcal/mol, corrected to 1000 °C) of Stone–Wales reactants (bottom, set to 0.0) and products (top) for pyracyclene derivatives. Values in parentheses are ZPE-corrected relative energies. Profile views (M06-2X/cc-pVDZ-optimized structures) are shown to the right of each species.

DOI: 10.1021/acs.joc.5b01274
J. Org. Chem. 2015, 80, 11718–11725

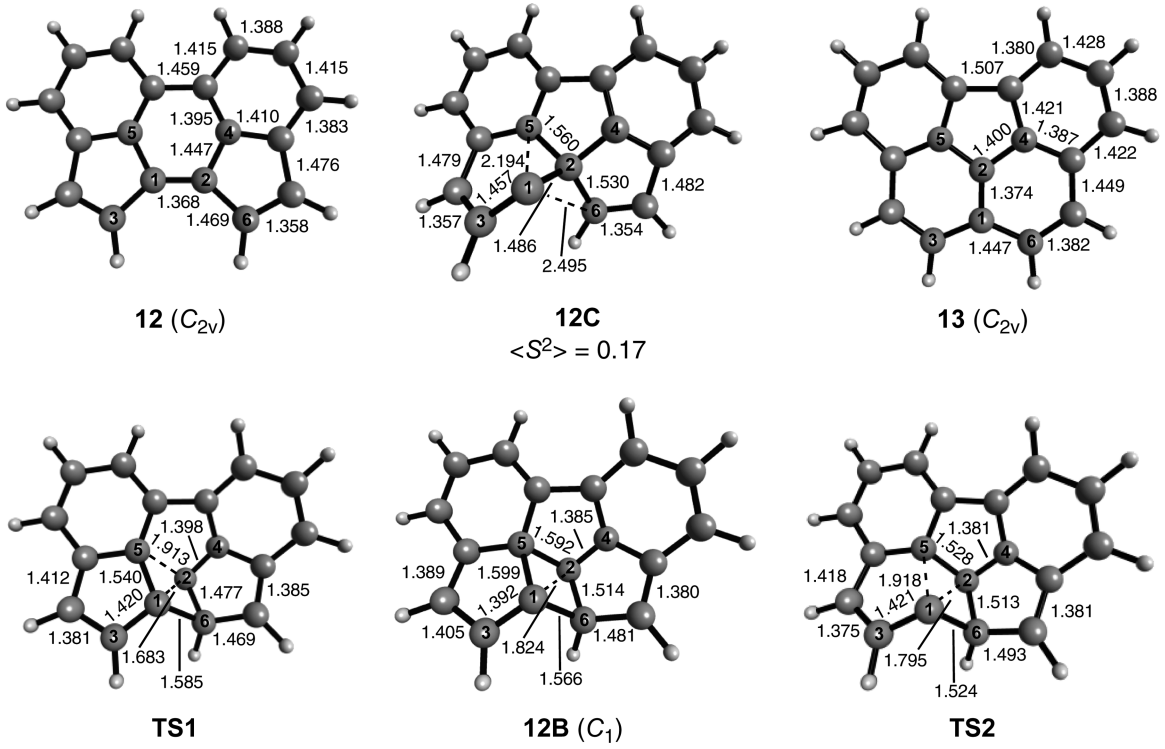

Figure 4. UM06-2X/cc-pVDZ-optimized geometries of stationary points in Stone–Wales rearrangement mechanisms connecting **12** and **13**. Distances in Å.

computed at high temperature due to the use of harmonic vibrational frequencies. For this reason, relative energies corrected for differences in zero point energies are also provided.

Density functional and BD(T) calculations were performed using Gaussian 09.[36] Structures were viewed with MacMolPlt,[37] and vibrational modes and orbitals were visualized with Molden.[38]

RESULTS AND DISCUSSION

Thermodynamics of the Reactions: Difficulty of Enclosing Pentagons. Before examining mechanisms, it is useful to consider the thermodynamics of the reactions. For *as*-indacene (**10**) and two of its derivatives, the net energetics are depicted in Figure 1. For these conversions, the number of pentagons decreases by one. Not surprisingly, conversion of *as*-indacene (**10**) to acenaphthylene (**11**) is highly exergonic due to the transformation of a quinoidal (and arguably antiaromatic) system into an aromatic one. Transformation of cyclopent[*hi*]acephenanthrylene (**12**) to benzo[*ghi*]-fluoranthene (**13**)[15] is predicted to still be exergonic, but less so than **10** → **11**, and formation of corannulene (**15**)[39−42] from dicyclopenta[*cd*,*fg*]pyrene (**14**)[43,44] is *endergonic* by 10.6 kcal/mol at 1000 °C (4.4 kcal/mol at 0 K). Thus, pyrolytic synthesis of corannulene via SWR of **14**, as was once suggested,[44] would not be feasible for thermodynamic reasons. The endergonic nature of **14** → **15** can be rationalized by noting the increase in curvature accompanying the reaction (Figure 1). Despite the tendency in some hydrocarbon rearrangements for perimeter five-membered rings to migrate toward more internal positions,[45−47] *completely surrounding* a 5-membered ring (i.e., generating a corannulene moiety and thus establishing or increasing curvature) significantly increases the strain in the system and renders the conversion thermodynamically unfavorable. This generalization is borne out by SWRs in pyracyclene derivatives (vide infra).

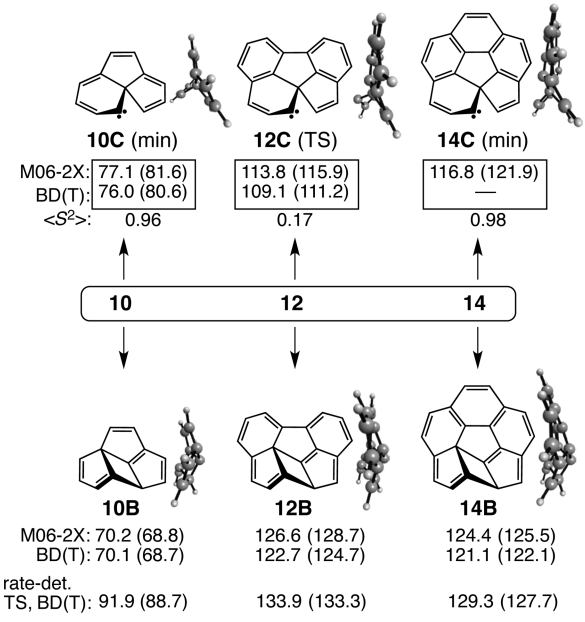

Figure 5. UM06-2X/cc-pVDZ and BD(T)/cc-pVDZ//UM06-2X/cc-pVDZ relative free energies (kcal/mol, corrected to 1000 °C) for carbenes (**C** suffixes) and cyclobutyl intermediates (**B** suffixes) connected to *as*-indacene (**10**) and two derivatives (**12** and **14**). Values in parentheses are ZPE-corrected relative energies. Carbenes **10C** and **14C** are intermediates ("min"), whereas **12C** is a transition state (TS). Profile views to the right of each structure show the nonplanarity of the species. Energies for the preferred pathway in each system are boxed. Relative free energies of the rate-determining transition states in the cyclobutyl mechanisms are given at bottom.

Figure 2 shows the reactants and products for the hypothetical SWRs of pyracyclene derivatives **16**, **18**, **19**, and **21**.

DOI: 10.1021/acs.joc.5b01274
J. Org. Chem. 2015, 80, 11718−11725

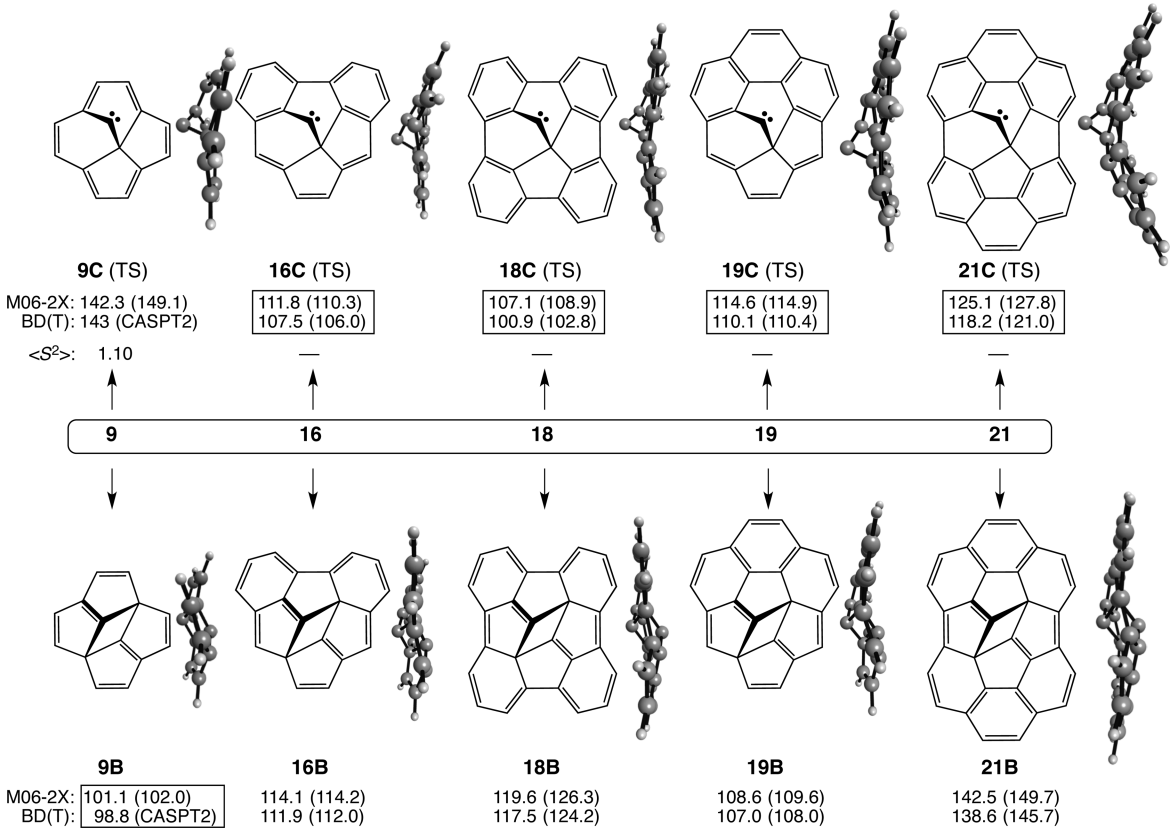

Figure 6. UM06-2X/cc-pVDZ and BD(T)/cc-pVDZ//UM06-2X/cc-pVDZ relative free energies (kcal/mol, corrected to 1000 °C) for carbenes (**C** suffixes) and cyclobutyl intermediates (**B** suffixes) connected to pyracyclene (**9**) and four derivatives (**16**, **18**, **19**, and **21**). Values in parentheses are ZPE-corrected relative energies. All carbenes here are transition states (TS). Profile views to the right of each structure show the nonplanarity of the species. Energies for the preferred pathway in each system are boxed. Pyracyclene (**9**) results in the BD(T) line are from ref 26 and were obtained at the CASPT2(14,14)/cc-pVDZ//UM06-2X/cc-pVDZ level because carbene **9C** was located as a ^{1}A″ state.

The hypothetical degenerate SWRs of **9** and diindeno[1,2,3,4-*defg*;1′,2′,3′,4′-*mnop*]chrysene (**18**)[48] are included to show the progressive increase in curvature in substrates and products. In the conversions in Figure 2, the number of pentagons remains constant. At one extreme, the SWR of dibenzopyracyclene isomers **16** → **17** is predicted to be 9−10 kcal/mol exergonic, very similar to **12** → **13**. Unlike **12** → **13**, the **16** → **17** transformation begins and ends with slightly curved structures. At the other extreme, conversion of **21**[49] to semibuckminsterfullerene **22**[50,51] is computed to be >17 kcal/mol endergonic and involves a significant increase in curvature resulting from the complete enclosure of two pentagons; the depth of the bowl[50] increases substantially from 2.00 Å in **21** to 2.72 Å in **22**. The somewhat anomalous case in this series is **19** → **20**,[51−53] a process involving complete enclosure of one pentagon; although it falls energetically between the other two cases, it is computed to be nearly thermoneutral despite its similarity to **14** → **15**.

Representative Mechanisms: Carbene and Cyclobutyl Routes. Beyond the issue of whether the SWRs under consideration are thermodynamically favorable or not, we primarily sought to elucidate the possible mechanisms. In searching for a concerted, dyotropic mechanism, all attempts to locate acetylenic transition states analogous to **A** (Scheme 5) failed. Stationary points resembling **A** were always computed to have multiple imaginary frequencies, indicating second- or higher-order saddle points. This contrasts with Bettinger's results on C_{60}, where such a transition state was located at the PBE/6-31G* and B3LYP/6-31G* level of theory.[12] These results will be discussed further below. Here, we will not consider radical-promoted or -catalyzed mechanisms in which initial H atom addition to a substrate is followed by rearrangement of a radical, which eventually loses H• to form product.[25,27]

We thus focused initially on carbene and cyclobutyl mechanisms, as such routes have been computed previously for pyracyclene and other systems.[25−27] Figure 3 shows these two pathways for the representative case of **12** → **13**. Figure 4 provides the optimized structures for the corresponding stationary points. The salient features of the structures are similar to those computed previously[26,27] for cases such as pyracyclene.

Mechanisms analogous to those in Figure 3 are found for all systems considered here, though some variations appear for different cases. For example, in most systems the carbene is a transition state, but in some it is an intermediate. In some of the cyclobutyl mechanisms, additional intermediates (e.g., benzvalenes) are found, but the highest-energy intermediates are always the cyclobutyl species. One common geometric feature is that all of the carbenes and cyclobutyl intermediates are significantly nonplanar. The carbene carbon consistently protrudes well out of the average plane of the molecule, and in all cyclobutyl intermediates (such as **12B**), the highly pyramidalized carbons C1 and C2 lie significantly above and below the average plane of the local *as*-indacene or pyracyclene perimeter. Another important generalization, for all the cyclobutyl mechanisms considered here, is that the rate-determining transition state is generally computed to be 11−22 kcal/mol higher in free energy (at 1000 °C) than the cyclobutyl intermediate. We can therefore

DOI: 10.1021/acs.joc.5b01274
J. Org. Chem. 2015, 80, 11718−11725

Scheme 7

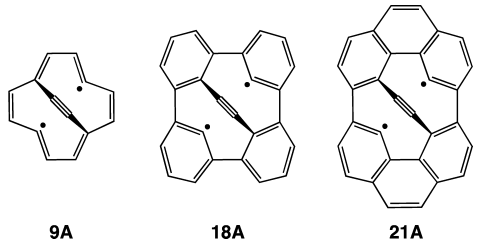

examine trends across series using the relative free energies of the cyclobutyl intermediate and carbene transition state (or intermediate) corresponding to each substrate. Figure 5 shows these results for the *as*-indacene series, and Figure 6 for the pyracyclene series. Figures 5 and 6 also provide profile views to show the nonplanarity of the carbene and cyclobutyl species.

The UM06-2X relative free energies for most carbene and cyclobutyl species are within 5 kcal/mol of those obtained with the BD(T) method. In addition, relative free energies of carbenes and cyclobutyl species at 1000 °C are within 7 kcal/mol of those computed at 0 K. For all systems in the *as*-indacene series (Figure 5), the lower-energy pathway is the carbene route if one accounts for the highest-energy transition state. In addition, only *as*-indacene (**10**) has $\Delta G^{\ddagger}$ (at 1273 K) <100 kcal/mol. Singlet carbenes **10C** and **14C** are predicted to be potential minima with the relevant (rate-determining) transition states lying ∼5 kcal/mol higher in both cases.

The preference for carbene pathways also dominates the pyracyclene series, as shown in Figure 6. Interestingly, from **9C** to **18C**, the relative energy of the carbene drops to 101−103 kcal/mol at the BD(T) level. Then, from **18C** to **21C**, the relative energy rises to 118−121 kcal/mol. Thus, for the pyracyclene-based series, **18C** is the most favorable carbene transition state with an energy on the border of feasibility. For comparison, Alder and Harvey found **18C** to lie 116 kcal/mol higher in energy than **18** at the B3LYP/6-31G* level.[25]

The corresponding cyclobutyl intermediates **16B**, **18B**, and **19B** have similar energies of 107−118 kcal/mol (Figure 6), though the flanking transition states are at least 10 kcal/mol higher. With the semibuckminsterfullerene species **21B**, the energy rises dramatically because the local C_i symmetry of the cyclobutyl moiety goes counter to the pronounced bowl-shaped nature of substrate **21**. In this series, pyracyclene appears to be the exception. Species **9B** is the most feasible cyclobutyl intermediate in this group because there is no curvature in the substrate to oppose the C_i symmetry in the intermediate. In addition, open-shell singlet (^{1}A″) carbene **9C** is computed to be much higher in energy than the other carbenes relative to the starting material.

Dyotropic Mechanisms via Acetylenic Diradicals? Given that carbene and cyclobutyl pathways exist, albeit with high activation energies, for the Stone−Wales rearrangements presented, it is worth considering the nature of the corresponding acetylene diradicals **A** and the potential for dyotropic mechanisms.[20] We chose acetylenes **9A**, **18A**, and **21A** for study, corresponding to SWRs of pyracyclene (**9**), diindenochrysene (**18**), and the $C_{30}H_{12}$ isomer **21**, respectively, as these represent the range of curvature covered in this work (Scheme 7).

In prior work using B3LYP/6-31G*, Alder and Harvey found that C_{2v}-symmetric **18A** is predicted to be a second-order saddle point in which the imaginary frequency at −1441 cm^{-1} corresponds to the Stone−Wales reaction coordinate and that

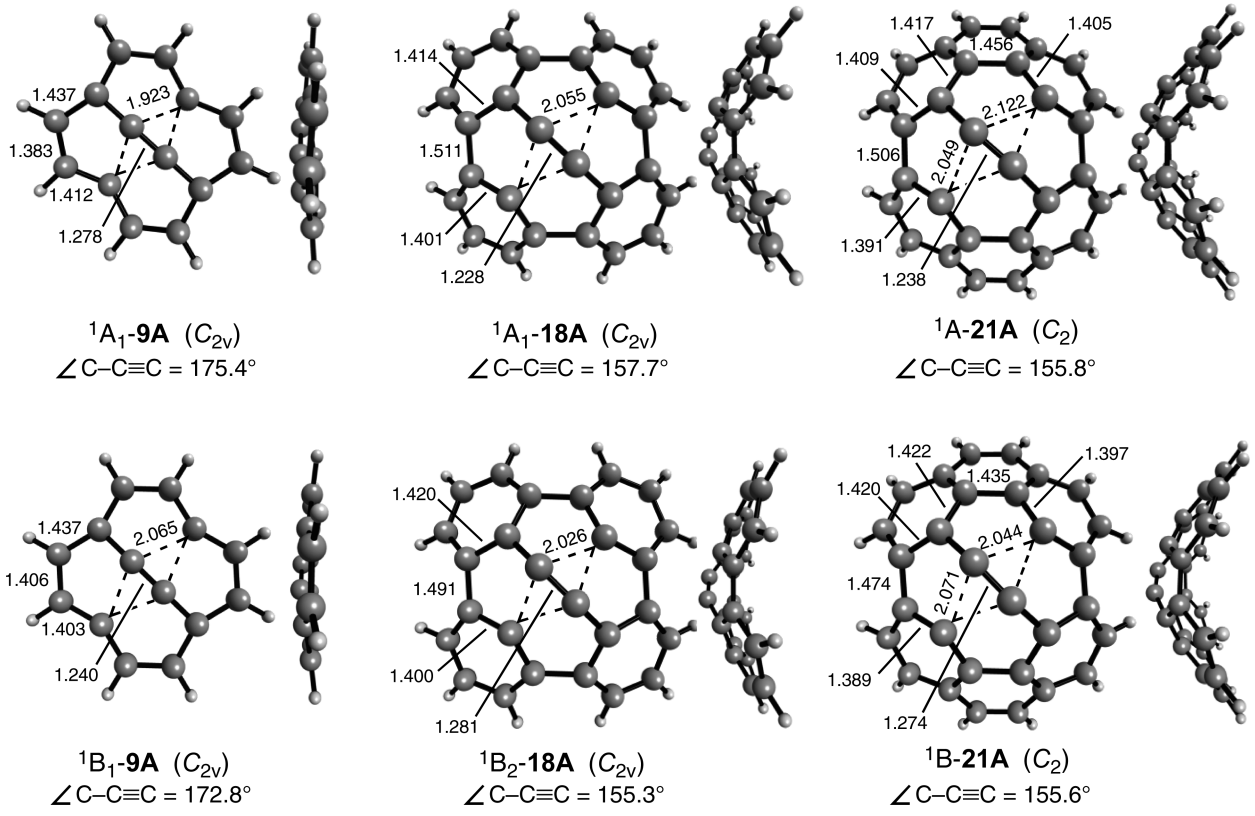

Figure 7. UM06-2X/cc-pVDZ-optimized structures of the two lowest singlet states of acetylenic diradicals **9A**, **18A**, and **21A**. Distances in Å.

DOI: 10.1021/acs.joc.5b01274
J. Org. Chem. 2015, 80, 11718−11725

357 cm^{-1} corresponds to deformation toward carbene **18C**.[25] They predicted that **18A** lies 192 kcal/mol above **18**.

Because of symmetry, a variety of electronic spin states are conceivable for the acetylenic diradicals. The UM06-2X-optimized structures for the two lowest singlet states of **9A**, **18A**, and **21A** are shown in Figure 7. Species **9A** and **18A** were optimized with C_{2v} symmetry and **21A** with C_2 symmetry.[54] In all three, the C≡C unit puckers out of the average plane of the pyracyclene perimeter surrounding it, as reflected in the C−C≡C angle: for example, 175.4° in $^1A_1$-**9A**, 157.7° in $^1A_1$-**18A**, and 155.8° in ^{1}A-**21A**. The distance from the formal radical centers and the acetylenic carbons ranges from 1.92 Å in $^1A_1$-**9A** to 2.12 Å in ^{1}A-**21A**.

Table 1 provides the relative energies and results of vibrational analyses for the acetylenic diradicals. The A states were computed by mixing the HOMO and LUMO, though in all three cases, the wave function converged to a closed-shell solution with $<S^2>$ = 0. In each case, the A state was computed to be more stable than the B state; however, in all cases, the A state was much higher than the corresponding carbene transition state and cyclobutyl intermediate. For example, $^1A_1$-**9A** is predicted to be ∼40 kcal/mol less stable than carbene **9C** and 80 kcal/mol less stable than **9B**.

Table 1. UM06-2X/cc-pVDZ Relative Energies (kcal/mol) and Imaginary Vibrational Frequencies for Two Lowest Singlet States of Acetylenic Diradicals 9A, 18A, and 21A[a]

species	sym	state	$<S^2>$	rel *E*	NIMAG	imaginary frequencies (cm^{-1})
$C_{14}H_8$						
$^1A_1$-**9A**	C_{2v}	$^1A_1$		182.1	3	b_2 −526 toward carbene **9C**
						a_2 −201 SWR rxn coordinate
						b_1 −92 C≡C side to side
$^1B_1$-**9A**	C_{2v}	$^1B_1$	1.04	185.4	4	a_2 −900 SWR rxn coordinate
						b_1 −599 C≡C side to side
						a_2 −483 perimeter π-bond shift
						b_2 −233 toward carbene **9C**
$C_{26}H_{12}$						
$^1A_1$-**18A**	C_{2v}	$^1A_1$		190.2	2	a_2 −1569 SWR rxn coordinate
						b_2 −387 toward carbene **18C**
$^1B_2$-**18A**	C_{2v}	$^1B_2$	1.04	198.8	3	b_2 −1071 toward carbene **18C**
						a_2 −966 SWR rxn coordinate
						b_1 −507 C≡C side to side
$C_{30}H_{12}$						
^{1}A -**21A**	C_2	^{1}A		186.9	2	a −1276 SWR rxn coordinate
						b −318 toward carbene **21C**
^{1}B-**21A**	C_2	^{1}B	1.04	201.2	2	a −872 SWR rxn coordinate
						b −506 C≡C side to side

[a]Energies of $C_{14}H_8$ isomers are relative to **9**, those of $C_{26}H_{12}$ isomers are relative to **18**, and those of $C_{30}H_{12}$ isomers are relative to **21**. Relative energies are corrected for ZPE differences. Wave functions of $^1B_1$, $^1B_2$, and ^{1}B states were obtained using the guess = alter option in Gaussian 09 and are thus "50:50" wave functions (i.e., 50% singlet, 50% triplet).

Feasibility. Only one transformation considered here—the hypothetical conversion of *as*-indacene (**10**) to acenaphthylene (**11**) via carbene **10C**—is predicted to be feasible under flash vacuum pyrolysis conditions, which can typically access temperatures up to 1100 or 1200 °C. An approximate criterion for such feasibility is that the free energy barrier must be less than ∼100 kcal/mol. This value is based on computed barriers for numerous high temperature rearrangements, including the topomerization of benzene; this reaction was observed by Scott et al. using isotopic labels at 1110 °C[55] and has a computed barrier of $\Delta G^{\ddagger}$ = 90−95 kcal/mol (at 1100 °C, for multiple possible mechanisms) at the CCSD(T) level of theory.[56,57] The hypothetical degenerate SWR of diindenochrysene (**18**) via carbene **18C** represents a borderline case with a computed barrier of just over 100 kcal/mol. Though most of the reactions considered here have computed free energy barriers of over 100 kcal/mol, some of them may still occur under conditions typical of the synthesis and annealing of fullerenes and carbon nanotubes. In addition, it is worth noting that, under conditions necessary to surmount barriers of ≥110 kcal/mol, C−H bond homolysis would occur because the C−H bond dissociation energies of aromatic hydrocarbons are ∼110−115 kcal/mol.[58−60] Scission of C−H bonds would generate hydrogen radicals and enable radical-promoted mechanisms that generally have lower barriers than the unimolecular mechanisms considered here.[25,27] Such mechanisms are under active investigation and will be the subject of a future report.

CONCLUSIONS

Carbene, cyclobutyl, and potential diradical mechanisms were studied computationally for Stone−Wales rearrangements in several derivatives of *as*-indacene (**10**) and pyracyclene (**9**). Free energies of reaction, obtained at the UM06-2X/cc-pVDZ and BD(T)/cc-pVDZ//UM06-2X/cc-pVDZ levels of theory, indicate that transformations involving an increase in curvature are thermodynamically unfavorable. In addition, the carbene transition states or intermediates are computed to be 100 to 120 kcal/mol higher than starting substrates, except for *as*-indacene (80 kcal/mol), which is the only substrate considered here that is predicted to have a barrier accessible under typical flash vacuum pyrolysis conditions. For pyracyclene derivatives, the relative free energy of cyclobutyl intermediates rises steadily with increasing curvature of the substrate. Singlet acetylenic diradicals **9A**, **18A**, and **21A** are predicted to be second- or higher-order saddle points and to lie far higher in energy than the corresponding carbenes and cyclobutyl species. Thus, up through semibuckminsterfullerene, such diradicals would not play a role in Stone−Wales rearrangements.

ASSOCIATED CONTENT

Supporting Information

The Supporting Information is available free of charge on the ACS Publications website at DOI: 10.1021/acs.joc.5b01274.

Results used to evaluate different basis sets; absolute energies, zero point energies, $<S^2>$ values, thermal corrections, and optimized Cartesian coordinates for all stationary points; and the complete citation for Gaussian 09 (PDF)

AUTHOR INFORMATION

Corresponding Authors

*E-mail: castroc@usfca.edu.

*E-mail: karney@usfca.edu.

Notes

The authors declare no competing financial interest.

ACKNOWLEDGMENTS

We thank the National Science Foundation (CHE-0910971, CHE-1213425) and the University of San Francisco Faculty Development Fund for generous financial support.

REFERENCES

(1) Gajewski, J. *Hydrocarbon Thermal Isomerizations*, 2nd ed.; Elsevier: New York, 2004.
(2) Ravindra, K.; Sokhi, R.; Van Grieken, R. *Atmos. Environ.* **2008**, *42*, 2895.
(3) Richter, H.; Howard, J. B. *Prog. Energy Combust. Sci.* **2000**, *26*, 565.
(4) Scott, L. T. *Pure Appl. Chem.* **1996**, *68*, 291.
(5) Scott, L. T. *Polycyclic Aromat. Compd.* **2010**, *30*, 247.
(6) *Carbon-Rich Compounds: From Molecules to Materials*; Haley, M. M., Tykwinski, R. R., Eds.; Wiley−VCH: Weinheim, 2006.
(7) Wiersum, U. E.; Jenneskens, L. W. In *Gas Phase Reactions in Organic Synthesis*; Vallée, Y., Ed.; Gordon and Breach: Australia, 1997; p 143.
(8) Stone, A. J.; Wales, D. J. *Chem. Phys. Lett.* **1986**, *128*, 501.
(9) Murry, R. L.; Strout, D. L.; Odom, G. K.; Scuseria, G. E. *Nature* **1993**, *366*, 665.
(10) Hawkins, J. M.; Nambu, M.; Meyer, A. *J. Am. Chem. Soc.* **1994**, *116*, 7642.
(11) Jin, Y.-f.; Hao, C. *J. Phys. Chem. A* **2005**, *109*, 2875.
(12) Bettinger, H. F.; Yakobson, B. I.; Scuseria, G. E. *J. Am. Chem. Soc.* **2003**, *125*, 5572.
(13) Ravinder, P.; Subramanian, V. *J. Phys. Chem. C* **2012**, *116*, 16815.
(14) Alder, R. W.; Whittaker, G. *J. Chem. Soc., Perkin Trans. 2* **1975**, 712.
(15) Dosa, P. I.; Schleifenbaum, A.; Vollhardt, K. P. C. *Org. Lett.* **2001**, *3*, 1017.
(16) Dosa, P. I.; Gu, Z.; Hager, D.; Karney, W. L.; Vollhardt, K. P. C. *Chem. Commun.* **2009**, 1967.
(17) Sarobe, M.; Flink, S.; Jenneskens, L. W.; Zwikker, J. W.; Wesseling, J. *J. Chem. Soc., Perkin Trans. 2* **1996**, *0*, 2125.
(18) Wiersum, U. E.; Jenneskens, L. W. *Tetrahedron Lett.* **1993**, *34*, 6615.
(19) Brown, R. F. C.; Choi, N.; Coulston, K. J.; Eastwood, F. W.; Wiersum, U. E.; Jenneskens, L. W. *Tetrahedron Lett.* **1994**, *35*, 4405.
(20) Reetz, M. T. *Angew. Chem., Int. Ed. Engl.* **1972**, *11*, 129.
(21) Fernández, I.; Cossío, F. P.; Sierra, M. A. *Chem. Rev.* **2009**, *109*, 6687.
(22) Woodward, R. B.; Hoffmann, R. *The Conservation of Orbital Symmetry*; Verlag Chemie: Weinheim, 1970.
(23) Zimmerman, H. E. *Acc. Chem. Res.* **1971**, *4*, 272.
(24) Some studies have probed radical-promoted mechanisms in which initial hydrogen atom addition to a substrate is followed by rearrangement of the resulting radical and subsequent loss of H to form product. Such mechanisms will not be considered here.
(25) Alder, R. W.; Harvey, J. N. *J. Am. Chem. Soc.* **2004**, *126*, 2490.
(26) Brayfindley, E.; Irace, E. E.; Castro, C.; Karney, W. L. *J. Org. Chem.* **2015**, *80*, 3825.
(27) Nimlos, M. R.; Filley, J.; McKinnon, J. T. *J. Phys. Chem. A* **2005**, *109*, 9896.
(28) Pastor, M. B.; Kuhn, A. J.; Nguyen, P. T.; Santander, M. V.; Castro, C.; Karney, W. L. *J. Phys. Org. Chem.* **2013**, *26*, 750.
(29) The sum of the three CCC angles = 346.4° relative to 328.5° for the corresponding sum in methane.
(30) Zhao, Y.; Truhlar, D. *Theor. Chem. Acc.* **2008**, *120*, 215.
(31) Dunning, T. H., Jr *J. Chem. Phys.* **1989**, *90*, 1007.
(32) Weigend, F.; Ahlrichs, R. *Phys. Chem. Chem. Phys.* **2005**, *7*, 3297.
(33) Dykstra, C. E. *Chem. Phys. Lett.* **1977**, *45*, 466.
(34) Handy, N. C.; Pople, J. A.; Head-Gordon, M.; Raghavachari, K.; Trucks, G. W. *Chem. Phys. Lett.* **1989**, *164*, 185.
(35) Kendall, R. A.; Dunning, T. H.; Harrison, R. J. *J. Chem. Phys.* **1992**, *96*, 6796.
(36) Frisch, M. J.; et al. *Gaussian 09*, revision D.01; Gaussian, Inc.: Wallingford, CT, 2009.
(37) Bode, B. M.; Gordon, M. S. *J. Mol. Graphics Modell.* **1998**, *16*, 133.
(38) Schaftenaar, G.; Noordik, J. H. *J. Comput.-Aided Mol. Des.* **2000**, *14*, 123.
(39) Barth, W. E.; Lawton, R. G. *J. Am. Chem. Soc.* **1966**, *88*, 380.
(40) Lawton, R. G.; Barth, W. E. *J. Am. Chem. Soc.* **1971**, *93*, 1730.
(41) Scott, L. T.; Cheng, P.-C.; Hashemi, M. M.; Bratcher, M. S.; Meyer, D. T.; Warren, H. B. *J. Am. Chem. Soc.* **1997**, *119*, 10963.
(42) Borchardt, A.; Fuchicello, A.; Kilway, K. V.; Baldridge, K. K.; Siegel, J. S. *J. Am. Chem. Soc.* **1992**, *114*, 1921.
(43) Sarobe, M.; Flink, S.; Jenneskens, L. W.; van Poecke, B. L. A.; Zwikker, J. W. *J. Chem. Soc., Chem. Commun.* **1995**, *0*, 2415.
(44) Scott, L. T.; Necula, A. *J. Org. Chem.* **1996**, *61*, 386.
(45) Scott, L. T.; Roelofs, N. H. *J. Am. Chem. Soc.* **1987**, *109*, 5461.
(46) Sarobe, M.; Jenneskens, L. W.; Wesseling, J.; Wiersum, U. E. *J. Chem. Soc., Perkin Trans. 2* **1997**, *0*, 703.
(47) Sarobe, M.; Jenneskens, L. W.; Wesseling, J.; Snoeijer, J. D.; Zwikker, J. W. *Liebigs Ann./Recueil* **1997**, *1997*, 1207.
(48) Bronstein, H. E.; Choi, N.; Scott, L. T. *J. Am. Chem. Soc.* **2002**, *124*, 8870.
(49) Hagen, S.; Bratcher, M. S.; Erickson, M. S.; Zimmermann, G.; Scott, L. T. *Angew. Chem., Int. Ed. Engl.* **1997**, *36*, 406.
(50) Rabideau, P. W.; Abdourazak, A. H.; Folsom, H. E.; Marcinow, Z.; Sygula, A.; Sygula, R. *J. Am. Chem. Soc.* **1994**, *116*, 7891.
(51) Sygula, A.; Rabideau, P. W. *J. Am. Chem. Soc.* **1999**, *121*, 7800.
(52) Abdourazak, A. H.; Sygula, A.; Rabideau, P. W. *J. Am. Chem. Soc.* **1993**, *115*, 3010.
(53) Sygula, A.; Abdourazak, A. H.; Rabideau, P. W. *J. Am. Chem. Soc.* **1996**, *118*, 339.
(54) For **9A**, we also considered a structure with a bond-alternating perimeter and only C_2 symmetry but optimization led to the C_{2v} structure with a bond-equalized perimeter.
(55) Scott, L. T.; Roelofs, N. H.; Tsang, T. H. *J. Am. Chem. Soc.* **1987**, *109*, 5456.
(56) Bettinger, H. F.; Schreiner, P. R.; Schaefer, H. F.; Schleyer, P. v. R. *J. Am. Chem. Soc.* **1998**, *120*, 5741.
(57) Madden, L. K.; Mebel, A. M.; Lin, M. C.; Melius, C. F. *J. Phys. Org. Chem.* **1996**, *9*, 801.
(58) Blanksby, S. J.; Ellison, G. B. *Acc. Chem. Res.* **2003**, *36*, 255.
(59) Reed, D. R.; Kass, S. R. *J. Mass Spectrom.* **2000**, *35*, 534.
(60) Barckholtz, C.; Barckholtz, T. A.; Hadad, C. M. *J. Am. Chem. Soc.* **1999**, *121*, 491.

DOI: 10.1021/acs.joc.5b01274
J. Org. Chem. 2015, 80, 11718−11725